Electronic Supplementary Information

Regioregular, Yet Ductile and Amorphous Indacenodithiophene-based Polymers with High-Mobility for Stretchable Plastic Transistors

Yongjoon Cho,[†,§] Sohee Park,[‡,§] Seonghun Jeong,[†] Heesoo Yang,[‡] Byongkyu Lee,[†] Sang Myeon Lee,[†] Byoung Hoon Lee,*[,‡] and Changduk Yang*[,†]

[†]*Department of Energy Engineering, School of Energy and Chemical Engineering, Perovtronics Research Center, Low Dimensional Carbon Materials Center, Ulsan National Institute of Science and Technology (UNIST), 50 UNIST-gil, Ulju-gun, Ulsan 44919, Republic of Korea.*
[‡]*Department of Chemical Engineering and Materials Science, Graduate Program in System Health Science and Engineering, Ewha Womans University, Seoul 03760, Republic of Korea*

Email: yang@unist.ac.kr, leebhoon@ewha.ac.kr

Table S1. Mobility, on/off current ratio, threshold voltage, LUMO/HOMO levels, molecular weight with PDI, channel length, and device structures of CDT- and IDT-based OFETs reported in the literature.

p-type polymers	Hole mobility [$cm^2\ V^{-1}\ s^{-1}$]	I_{on}/I_{off}	V_T [V]	LUMO/HOMO [eV]	Mn [kDa]/ PDI	Channel length [μm]	Device structure	Ref.
P_C1	1.4	6.3×10^2	10.1	-3.55/ -4.80	68/ 3.6	80 or 160	BG/ BC	1
P_C2	0.3	2.8×10	9.6	-3.89/ -5.19	67/ 4.1	80 or 160	BG/ BC	1
P_C3	0.62	1.4×10^4	-1.9	-3.15/ -4.98	23.5/ 2.47	80	BG/ BC	2
P_C4	1.45	2.2×10^4	-1.3	-3.11/ -5.00	23.1/ 2.45	80	BG/ BC	2
P_C5	1.2	5.5×10	14.6	-3.78/ -5.03	62/ 3.4	80 or 160	BG/ BC	1
P_C6	5×10^{-3}	1×10^4	N/A	-3.69/ -5.23	40/ 2.5	20	BG/ TC	3

P_C7	0.4	2×10^3	N/A	-3.70/ -5.07	28/ 1.9	20	BG/ TC	3
P_C8	0.6	2×10^4	N/A	-3.70/ -5.16	34/ 3.1	20	BG/ TC	3
P_C9	1.05×10^{-3}	10^4	-2	-3.04/ -4.88	16.2/ 2.55	50	BG/ TC	4
P_C10	4.3×10^{-4}	2.4×10^3	-6.2	-3.0/ -5.1	23/ 2.4	80 or 160	BG/ BC	5
P_C11	1.1	9.8×10^5	1.6	-3.25/ -5.30	34/ 2.0	80 or 160	BG/ BC	6
P_C12	1.0	1.4×10^6	7.1	-3.31/ -5.25	28/ 2.1	80 or 160	BG/ BC	6
P_C13	5.8×10^{-3}	1.6×10^4	-19.1	-3.1/ -5.2	25/ 2.4	80 or 160	BG/ BC	5
P_C14	1.1	1.3×10^6	4.2	-3.34/ -5.30	33/ 2.3	80 or 160	BG/ BC	6
P_C15	3.7×10^{-4} (electron mobility)	10^2	22	-3.70/ -5.25	21.8/ 1.4	60	BG/ TC	7
P_I1	3.6	10^6	N/A	-3.7/ -5.4	80/ 2	20	TG/ BC	8
P_I2	0.09	$3 \times 10^6 \pm 2 \times 10^6$	N/A	-3.32/ -5.58	15/ 1.7	50	BG/ TC	9
P_I3	0.3	$6 \times 10^4 \pm 3 \times 10^4$	N/A	N/A	14/ 1.6	50	BG/ TC	9
P_I4	5.01	2×10^6	-62	-3.21/ -5.45	138/ 1.98	70	TG/ BC	10
P_I5	6.1×10^{-2}	10^4-10^5	-19	-3.39/ -5.31	51.9/ 1.43	40	BG/ TC	11
P_I6	4.9×10^{-4} (electron mobility)	10^2-10^3	38	-3.67/ -5.34	47.3/ 1.72	40	BG/ TC	11
P_I7	0.2	$>10^6$	-19	N/A/ -5.4	64/ 2.63	20	TG/ BC	12
P_I8	0.07 (avg.)	$\sim 10^6$	-9	-3.45/ -5.47	29/ 1.52	N/A	TG/ BC	13
P_I9	0.03 (avg.)	$\sim 10^6$	-10	-4.05/ -5.43	20/ 1.45	N/A	TG/ BC	13

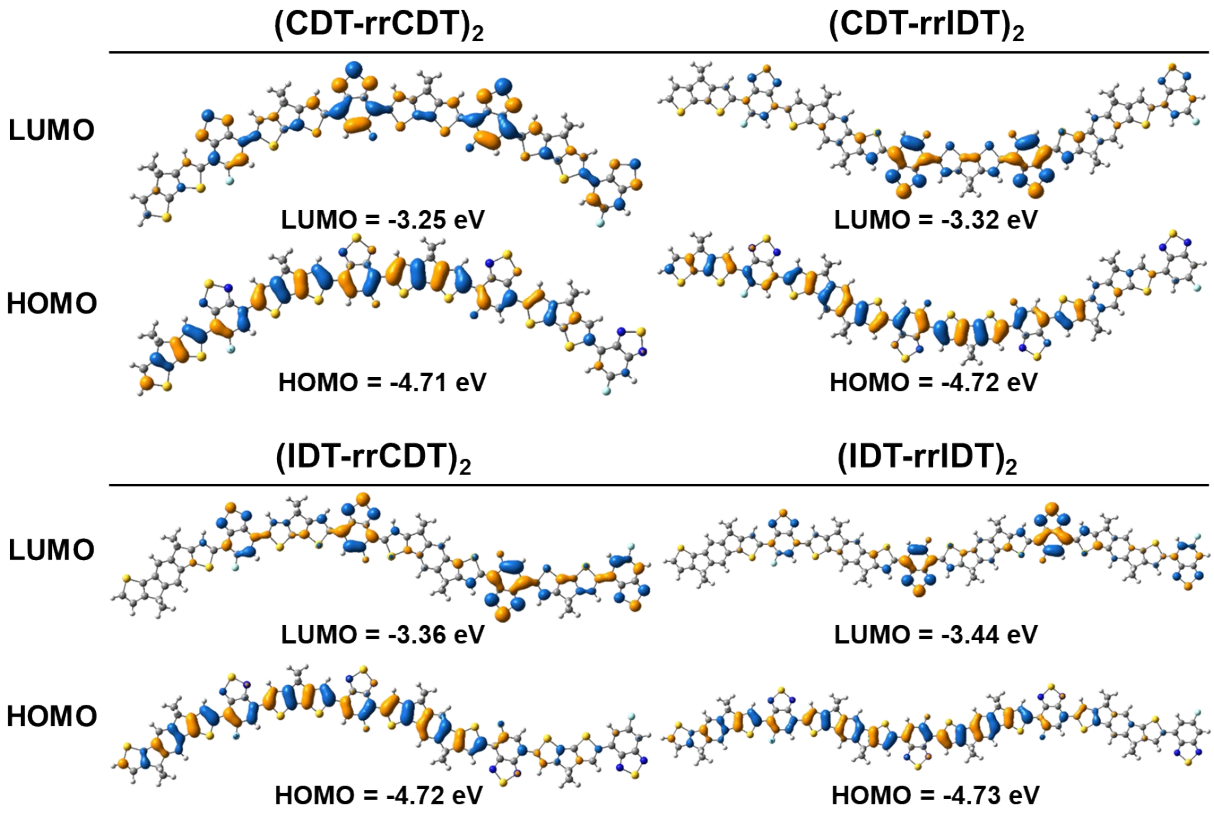

Figure S1. Simulated HOMO and LUMO orbitals of the dimers by DFT calculation.

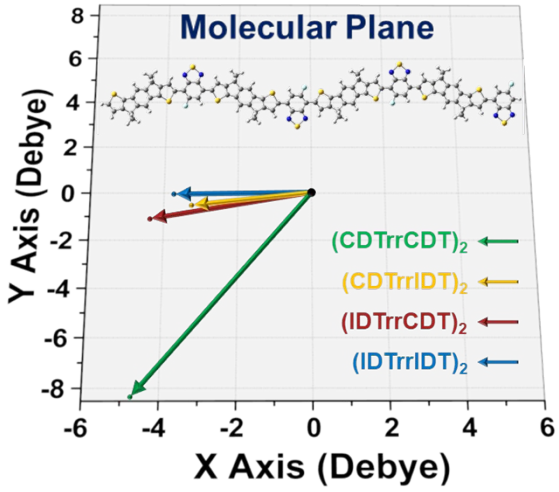

Figure S2. Dipole momentum of the dimeric repeating units calculated by DFT (the XY-plane represents the molecular planes).

Table S2. Calculated dipole moments and energy levels of the dimers sequenced with $(CDT\text{-}rrCDT)_2$, $(CDT\text{-}rrIDT)_2$, $(IDT\text{-}rrCDT)_2$, and $(IDT\text{-}rrIDT)_2$.

	Vector			Dipole Moment [D]	E_{HOMO}^{DFT} [eV]	E_{LUMO}^{DFT} [eV]
	x	y	z			
$(CDT\text{-}rrCDT)_2$	-4.74	-8.37	0.00	9.62	-4.71	-3.25
$(CDT\text{-}rrIDT)_2$	-3.28	-0.52	0.00	3.32	-4.72	-3.32
$(IDT\text{-}rrCDT)_2$	-4.38	-1.10	0.00	4.51	-4.72	-3.36
$(IDT\text{-}rrIDT)_2$	-3.63	-0.04	0.00	3.63	-4.73	-3.44

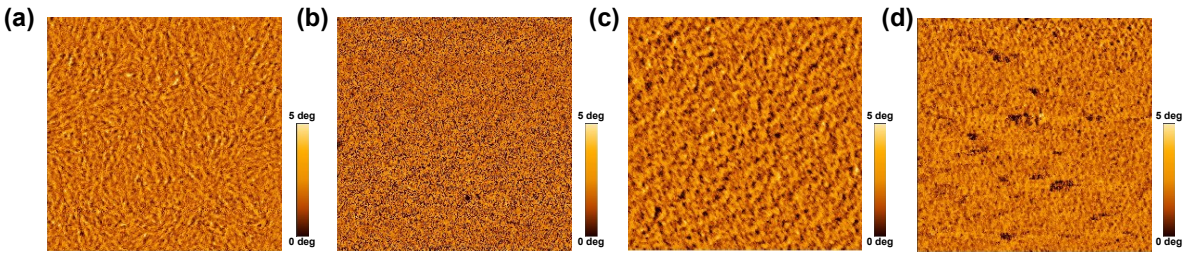

Figure S3. AFM phase images of (a) P1, (b) P2, (c) P3, and (d) P4 thin films annealed at optimized temperatures (2 μm × 2 μm in size).

Table S3. GIWAXS parameters of P1, P2, P3, and P4 annealed under optimized temperatures.

	Out-of-Plane						In-Plane								
	π-π stacking cell axis (010)			lamellar stacking cell axis (100)			π-π stacking cell axis (010)			backbone stacking (001)			lamellar stacking cell axis (100)		
	q [Å^{-1}]	d-spacing [Å]	CCL [nm]	q [Å^{-1}]	d-spacing [Å]	CCL [nm]	q [Å^{-1}]	d-spacing [Å]	CCL [nm]	q [Å^{-1}]	d-spacing [Å]	CCL [nm]	q [Å^{-1}]	d-spacing [Å]	CCL [nm]
P1		N/A		0.262	24.0	26.8	1.76	3.57	5.10		N/A			N/A	
P2	1.54	4.08	1.65	0.262	24.0	13.6		N/A			N/A		0.256	24.5	9.81
P3	1.55	4.06	1.55	0.261	24.1	11.6		N/A			N/A		0.257	24.4	10.7
P4	1.54	4.08	1.51	0.260	24.2	8.83		N/A		0.394	15.959	15.3		N/A	

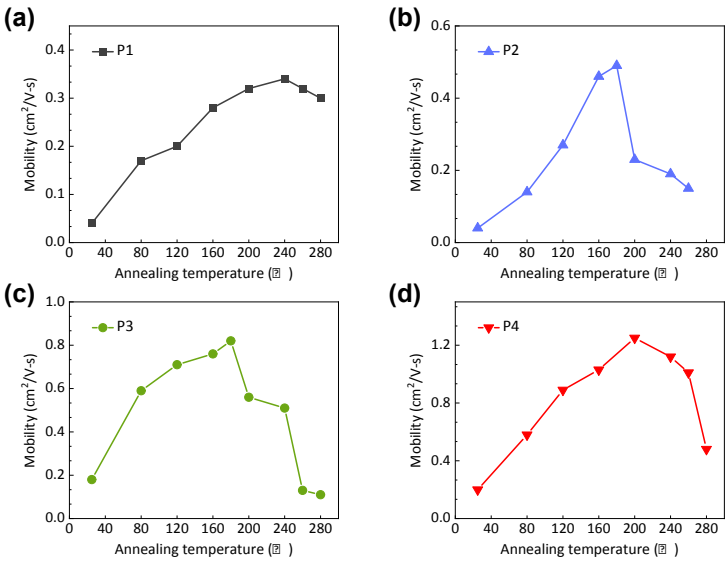

Figure S4. Mobility variation of OFETs with annealed (a) P1, (b) P2, (c) P3, and (d) P4 thin films obtained at various annealing temperatures.

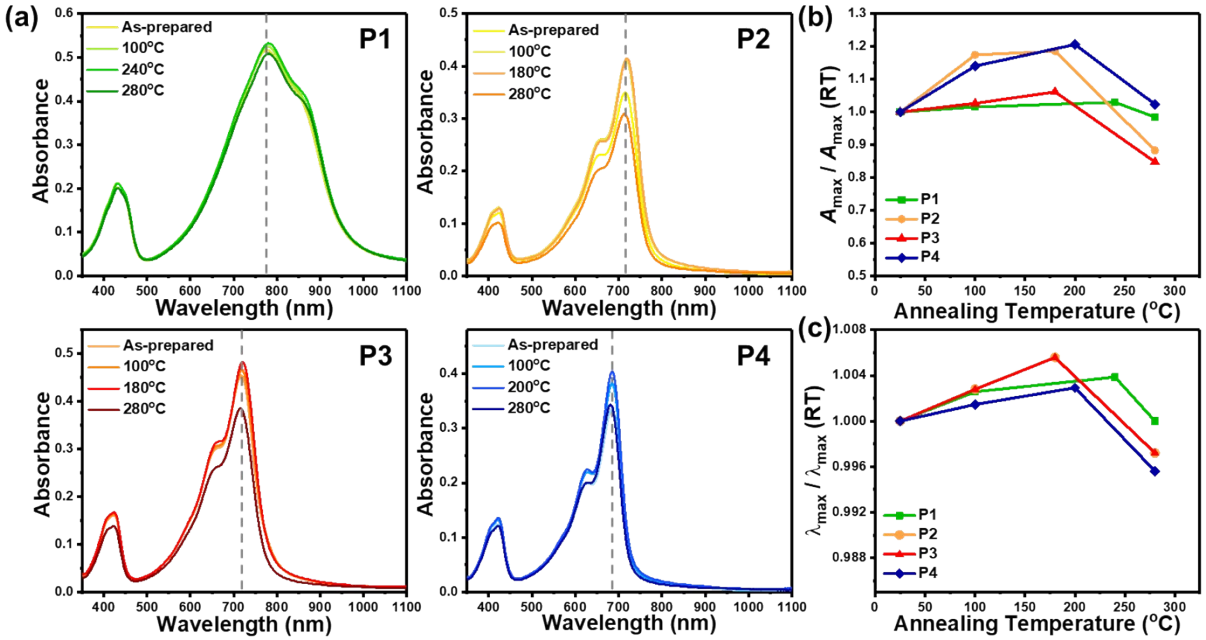

Figure S5. (a) UV–Vis absorption spectra of P1–P4 thin films at various thermal annealing temperatures (25–280℃). Changes in (b) absorbance and (c) λ_{max} of thermal annealed P1–P4 thin films relative to pristine thin films.

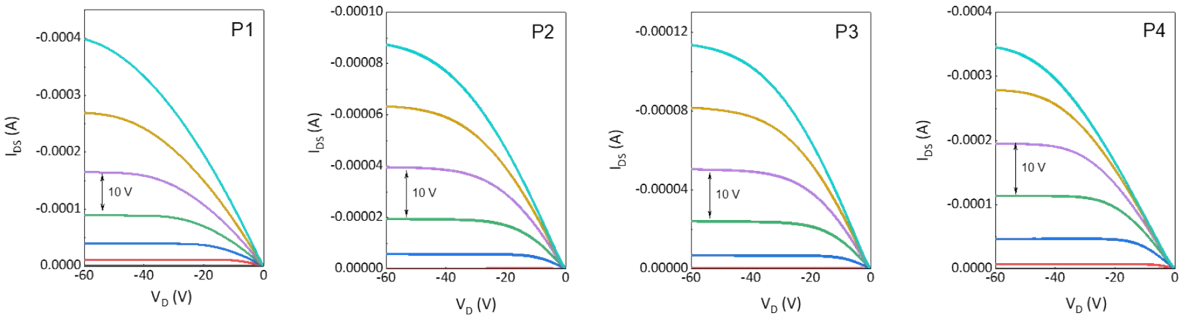

Figure S6. Output characteristics of the BGTC devices with MoO_3/Au source and drain electrodes.

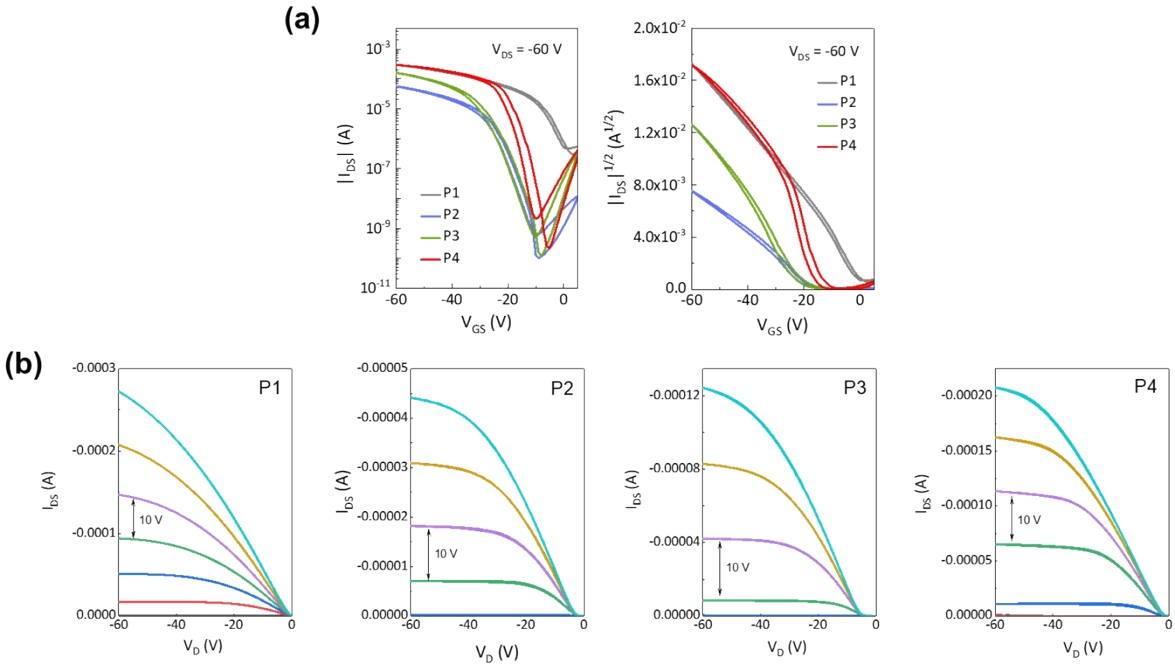

Figure S7. (a) Transfer characteristics and (b) output characteristics of the BGTC devices with Au as source and drain electrodes.

Table S4. Device parameters of OFETs fabricated with Au contact electrodes.

Polymer	μ_{max} [$cm^2\ V^{-1}\ s^{-1}$]	μ_{ave}* [$cm^2\ V^{-1}\ s^{-1}$]	V_T [V]	On/Off Ratio
P1	0.44	0.32 (0.09)	8.4	5.75×10^2
P2	0.22	0.20 (0.01)	-18.5	5.65×10^5
P3	0.60	0.46 (0.09)	-20.6	1.40×10^6
P4	2.22	1.74 (0.31)	-14.0	4.54×10^5

*The values indicate average mobility obtained from the 10 independent OFETs, where the numbers in parentheses indicate standard deviation of the average mobility.

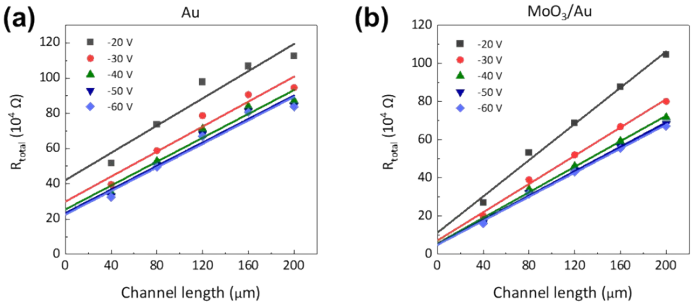

Figure S8. Total resistance of the BGTC P4-OFETs without (a) or with (b) MoO_3 electron blocking layers.

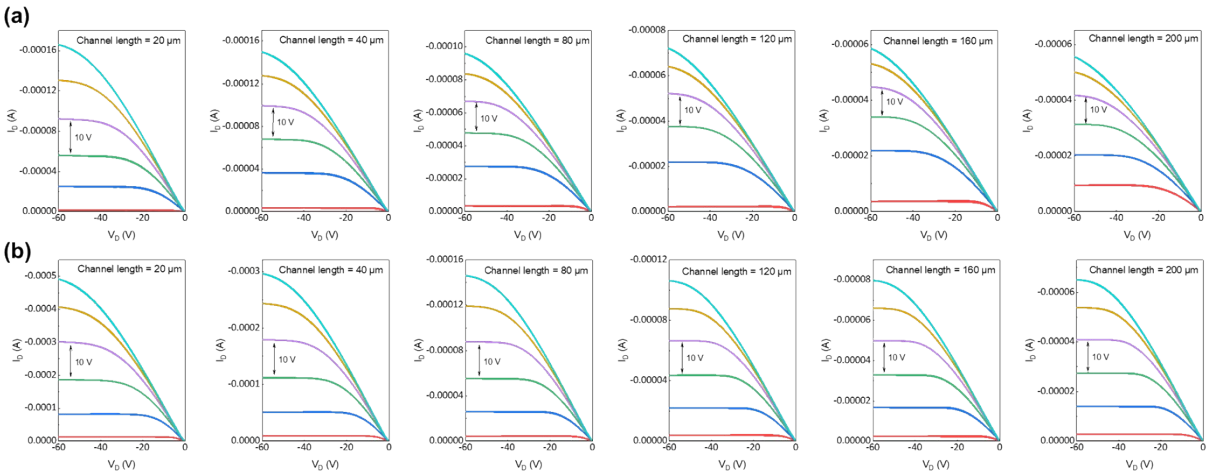

Figure S9. Output characteristics of the BGTC P4-OFETs without (a) and with (b) MoO_3 interfacial layers with varying channel length.

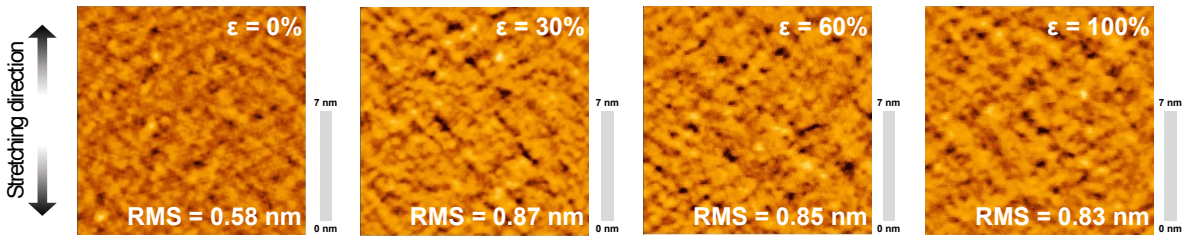

Figure S10. AFM topographic images and RMS roughness values of P3 thin films before and after elongation at various strain values (ε = 0, 30, 60, and 100%). Size: 2 μm × 2 μm.

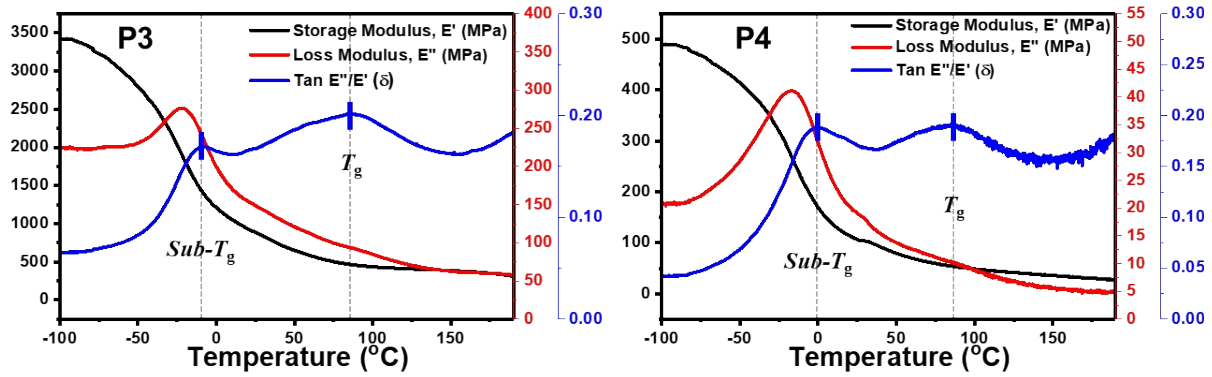

Figure S11. DMA measurement results of the storage modulus, loss modulus, and tan (δ) of P3 and P4.

Table S5. Sub-T_g and T_g of P3 and P4.

Polymer	*sub*-T_g[a] [°C]	T_g[a] [°C]
P3	-8.7	84.9
P4	-0.4	86.8

Table S6. Previously reported ductile polymers and their crystalline nature, origin of ductility, molecular weight, polydispersity index, charge-carrier mobility, elastomeric substrate, and crack-onset strain.

Polymer	Crystalline nature	Reason for ductility	Number-average molecular weight [kDa]/PDI	Mobility [$cm^2 V^{-1} s^{-1}$]	Elastomeric substrate	Crack-onset strain [%]	Reference
P2	Near-amorphous	Amorphous domain, sliding of polymer chains	90.3 / 1.43	0.49	PDMS	30	
P3	Near-amorphous	Amorphous domain, sliding of polymer chains	84.0 / 1.50	1.13	PDMS	100	**This work**
P4	Near-amorphous	Amorphous domain, sliding of polymer chains	93.5 / 1.80	4.13	PDMS	60	
$PDPP_{urethane}$-TT	Semicrystalline	Secondary bonding	154 / 1.15	2.58×10^{-2}	PMDS	50	14
$PDPP_{urethane}$-BT	Semicrystalline	Secondary bonding	164 / 1.12	3.46×10^{-2}	PDMS	75	14
$PDPP_{urethane}$-TVT	Semicrystalline	Secondary bonding	171 / 1.10	3.90×10^{-2}	PDMS	100	14
T-50	Near-amorphous	Flexible segment	25.7 / 3.2	$\sim 2 \times 10^{-2}$	PDMS	100	15
T-75	Near-amorphous	Flexible segment	22.9 / 3.5	$\sim 2 \times 10^{-2}$	PDMS	100	15
TT-50	Near-amorphous	Flexible segment	25.9 / 4.1	$\sim 1 \times 10^{-1}$	PDMS	100	15
P4	Semicrystalline	Amorphous domain, Twisted orientation	126 / 3.00	1.39	PDMS	60-100	16
P5	Semicrystalline	Amorphous domain, Twisted orientation	146 / 3.27	0.84	PDMS	60-100	16
P6	Semicrystalline	Amorphous domain, Twisted orientation	158 / 3.57	1.27	PDMS	60-100	16

P3HT (regioregular)	Semicrystalline	Conformational disorder of side chains	62 / 1.9	0.07	PDMS	150	17, 18
rr PHT (regiorandom P3HT)	Amorphous	Amorphous domain	14.8 / 3.50	N/A	Ecoflex	100	19
P3	Semicrystalline	Soft amorphous domain, Entanglement of nanofibers	29.5 / 1.69	$\sim 2 \times 10^{-1}$	PDMS	40	20
20DPPTTECx	Semicrystalline	Crosslinking	16.5 / 4.00	0.91	PDMS	>150	21
DBB-DPP	Semicrystalline	Amorphous domain, Flexible segment	24.7 / 2.99	~1.80	PDMS	30	22
C6-DPP	Semicrystalline	Amorphous domain, Flexible segment	40.0 / 2.93	~2.30	PDMS	45	22
C12-DPP	Semicrystalline	Amorphous domain, Flexible segment	31.8 / 32.6	~1.50	PDMS	100	22
IDTBT	Near-amorphous	Amorphous domain, Sliding of polymer chains	108.6 / 2.7	1.8	PDMS	130	23
PDPP-TT-PDMS-25k	Near-amorphous	Elastomeric segment	9.50 / 2.53	0.08	PDMS	85	24
PII2T	Semicrystalline	High free volume by long branched alkyl chain	N/A	1.49×10^{-1}	PDMS	100	25
PIDTBT (low Mw)	Near-amorphous	Near-amorphous	57 / 2.9	0.65	PDMS	30	26
PIDTBT (medium Mw)	Near-amorphous	Near-amorphous	100 / 2.8	1.65	PDMS	60	26
PIDTBT (High Mw)	Near-amorphous	Near-amorphous, High molecular weight	112 / 3.0	2.17	PDMS	102	26
RP33	Near-amorphous	Amorphous domain	16.1 / 1.15	1.37	PDMS	40	27

PIDTBPD	Near-amorphous	Amorphous domain	15 / 1.7	0.09	PDMS	100	9
			18 / 2.2	3×10^{-3}	PDMS	40	28
PII2T-C6	Semicrystalline	Floppy side chain	305 / 3.3	3.22	PDMS	60	29
PII2T-C8	Semicrystalline	Floppy side chain	434 / 1.6	8.06	PDMS	100	29
PII2T-PBA10	Near-Amorphous	Soft and elastic side chain	133 / 2.5	0.22	PDMS	40	30
PII2T-PBA20	Near-Amorphous	Soft and elastic side chain	49.6 / 2.6	0.063	PDMS	60	30
PII2T-PBA100	Only-Amorphous	Soft and elastic side chain	6.9 / 1.3	$<10^{-7}$	PDMS	100	30
P2	Semicrystalline	Amorphous domain, secondary bonding	19.7 / 3.3	1.62	PDMS	30	31
P3	Semicrystalline	Amorphous domain, secondary bonding	16.2 / 3.0	1.32	PDMS	110	31
P4	Semicrystalline	Amorphous domain, secondary bonding	35.5 / 2.6	0.58	PDMS	120	31
P3	Semicrystalline	Amorphous domain, secondary bonding	55 / 2.33	0.31	PDMS	60	32
P4	Semicrystalline	Amorphous domain, secondary bonding	40.8 / 2.22	0.073	PDMS	60	32

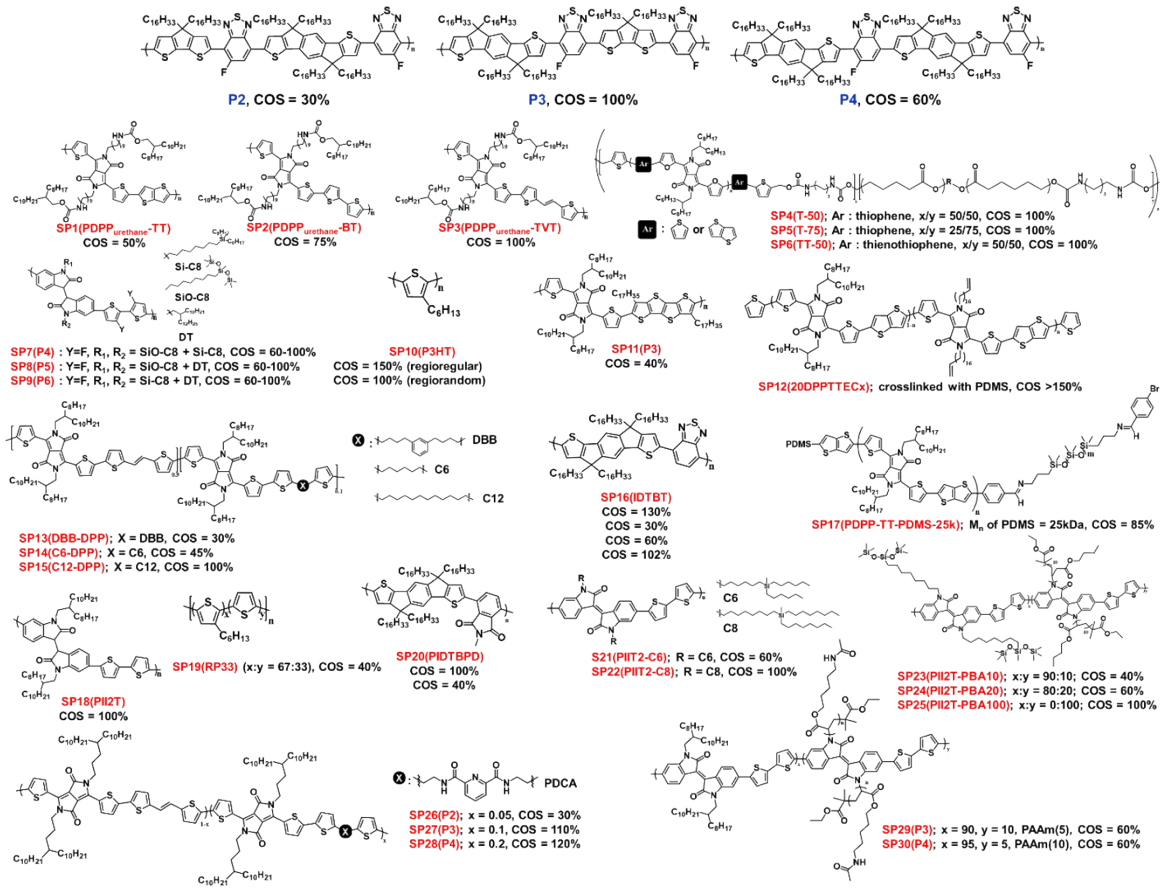

Figure S12. Chemical structures and crack-onset strains of P2, P3, and P4 in this work and previously reported ductile polymers.

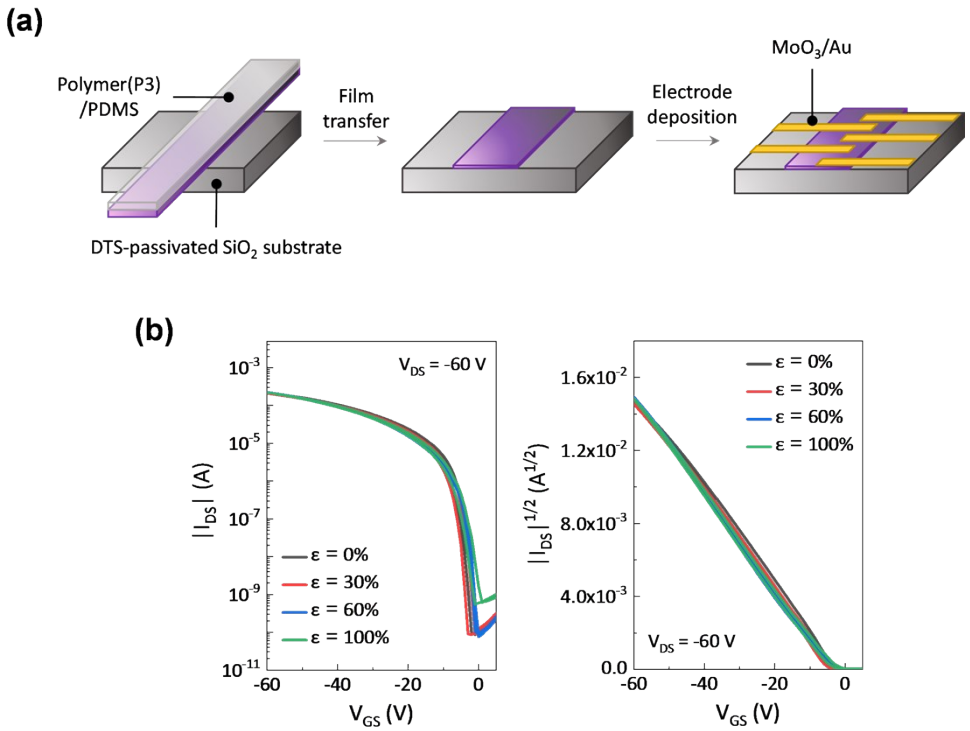

Figure S13. (a) Schematic illustration of device fabrication process using stretched P3 thin films by dry transfer process, (b) transfer characteristics of the P3 devices at various strain values (ε = 30, 60, and 100%). The transfer curve for ε = 0% was obtained from the device fabricated with a transferred P3 thin film without elongation.

Table S7. Device parameters of P3-OFETs at various strain values.

Strain (ε, %)	μ_{max} ($cm^2\ V^{-1}\ s^{-1}$)	μ_{ave}* ($cm^2\ V^{-1}\ s^{-1}$)	V_T (V)	On/Off Ratio
0	0.27	0.26 (0.01)	-1.42	2.60×10^6
30	0.27	0.27 (0.01)	-2.88	2.33×10^6
60	0.30	0.26 (0.03)	-5.92	2.93×10^6
100	0.35	0.30 (0.05)	-4.74	3.60×10^5

*The values indicate average mobility obtained from the 4 independent OFETs, where the numbers in parentheses indicate standard deviation of the average mobility.

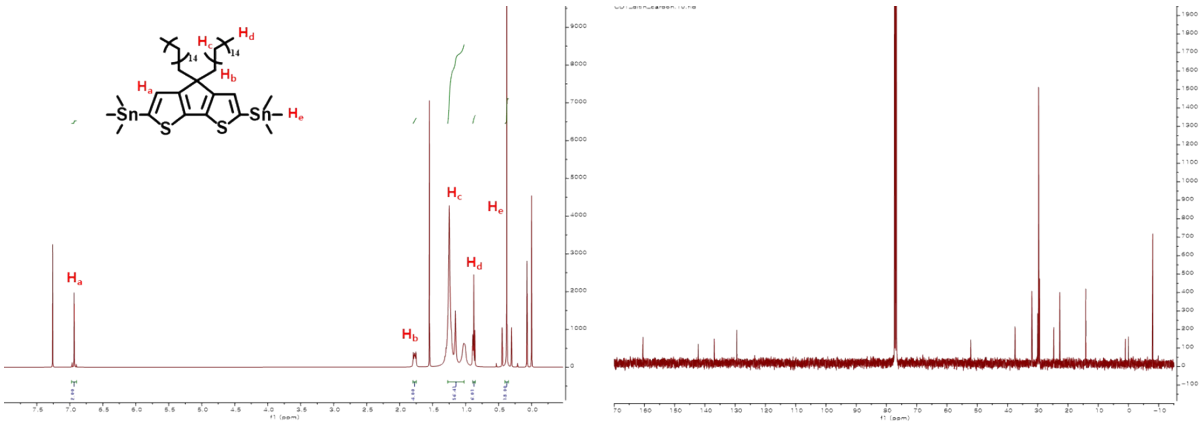

Figure S14. ^{1}H NMR and ^{13}C NMR data of M1.

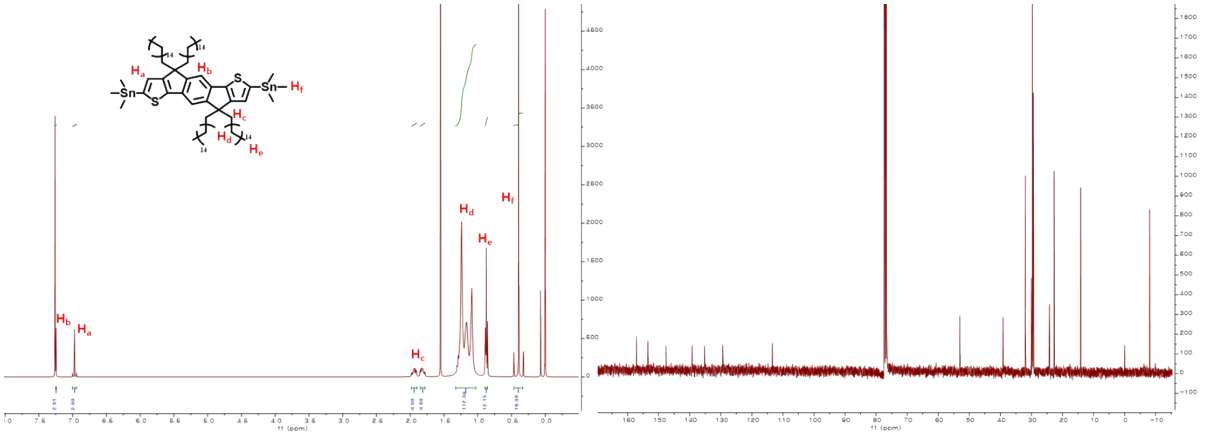

Figure S15. ^{1}H NMR and ^{13}C NMR data of M3.

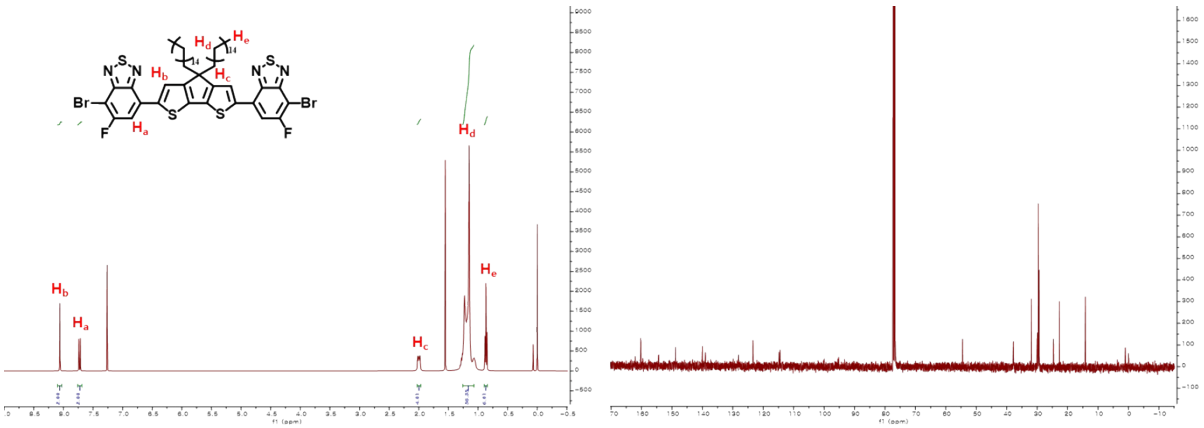

Figure S16. ^{1}H NMR and ^{13}C NMR data of M2.

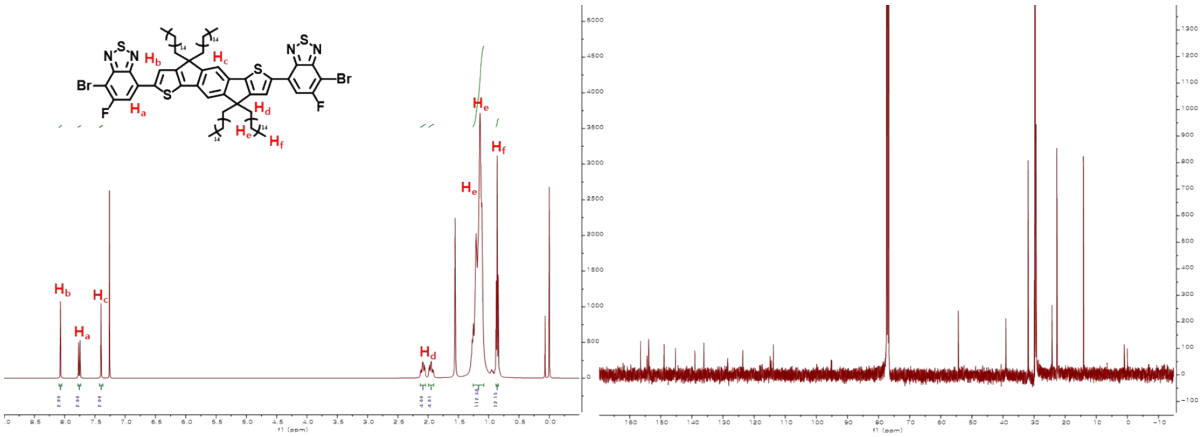

Figure S17. ^{1}H NMR and ^{13}C NMR data of M4.

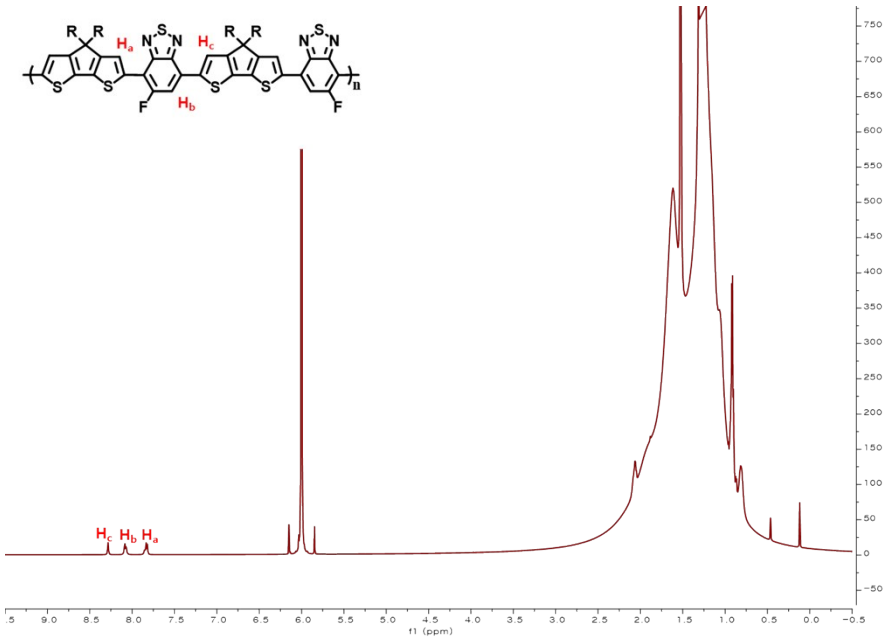

Figure S18. ^{1}H NMR data of P1.

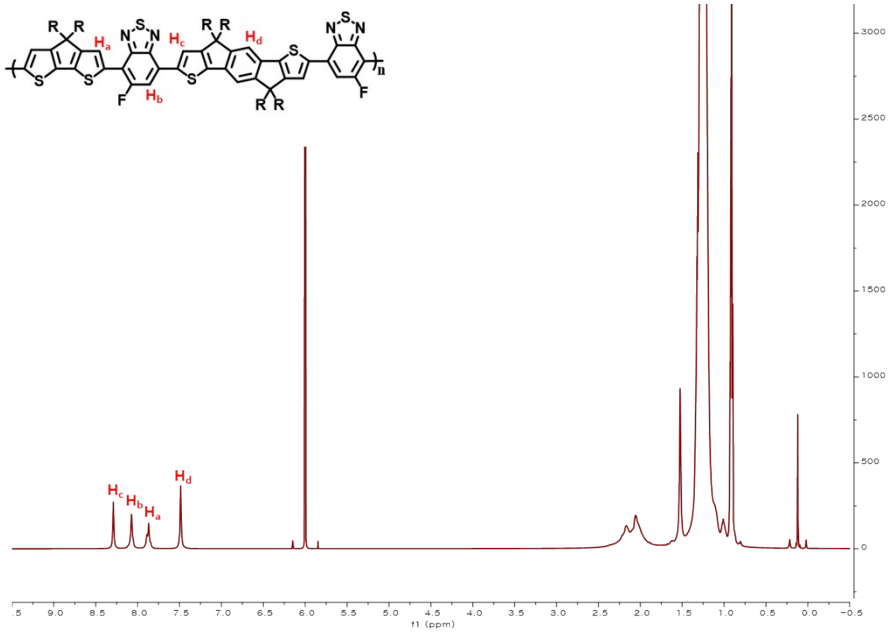

Figure S19. ^{1}H NMR data of P2.

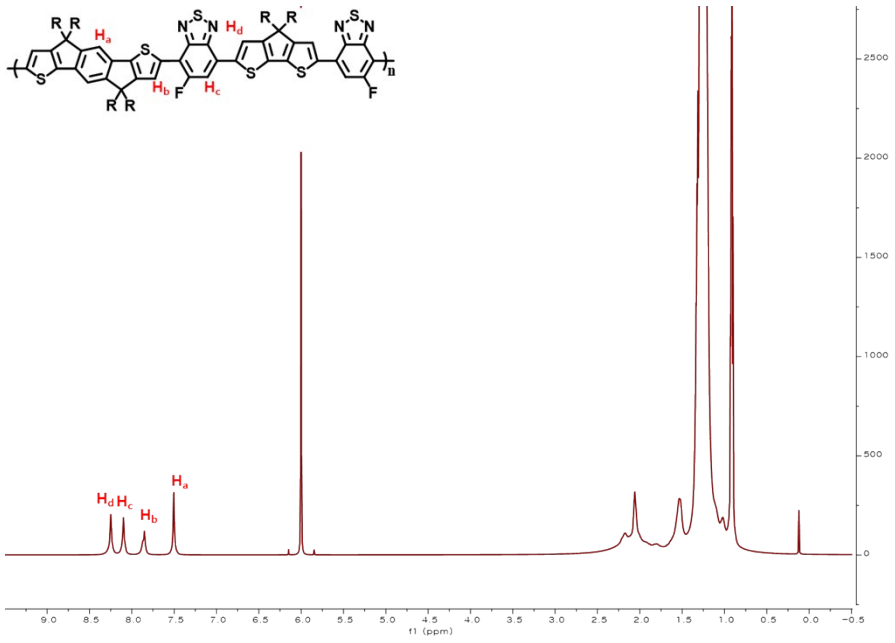

Figure S20. ^{1}H NMR data of P3.

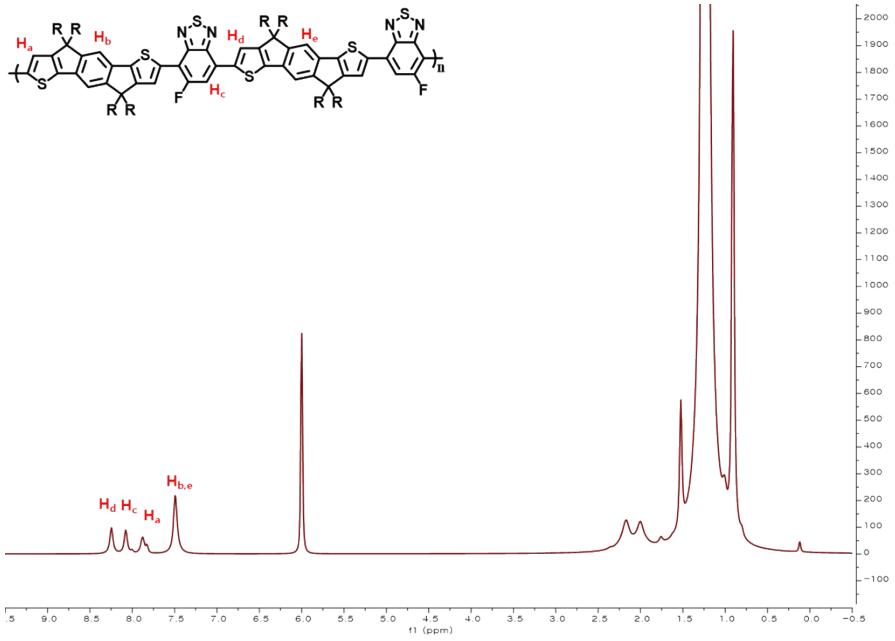

Figure S21. ^{1}H NMR data of P4.

References

1. M. Wang, M. Ford, H. Phan, J. Coughlin, T.-Q. Nguyen and G. C. Bazan, *Chem. Commun.*, 2016, **52**, 3207-3210.
2. G.-J. N. Wang, L. Shaw, J. Xu, T. Kurosawa, B. C. Schroeder, J. Y. Oh, S. J. Benight and Z. Bao, *Adv. Funct. Mater.*, 2016, **26**, 7254-7262.
3. J. Lee, S. H. Kang, S. M. Lee, K. C. Lee, H. Yang, Y. Cho, D. Han, Y. Li, B. H. Lee and C. Yang, *Angew. Chem. Int. Ed. Engl.*, 2018, **57**, 13629-13634.
4. L. Ying, B. B. Hsu, H. Zhan, G. C. Welch, P. Zalar, L. A. Perez, E. J. Kramer, T. Q. Nguyen, A. J. Heeger, W. Y. Wong and G. C. Bazan, *J. Am. Chem. Soc.*, 2011, **133**, 18538-18541.
5. P. K. Madathil, S. Cho, S. Choi, T.-D. Kim and K.-S. Lee, *Macromol. Res.*, 2018, **26**, 934-941.
6. M. Wang, M. J. Ford, A. T. Lill, H. Phan, T. Q. Nguyen and G. C. Bazan, *Adv. Mater.*, 2017, **29**, 1603830.
7. M. Wang, M. J. Ford, C. Zhou, M. Seifrid, T. Q. Nguyen and G. C. Bazan, *J. Am. Chem. Soc.*, 2017, **139**, 17624-17631.
8. C.-H. Li, J. Kettle and M. Horie, *Mater. Chem. Phys.*, 2014, **144**, 519-528.
9. X. Zhang, H. Bronstein, A. J. Kronemeijer, J. Smith, Y. Kim, R. J. Kline, L. J. Richter, T. D. Anthopoulos, H. Sirringhaus, K. Song, M. Heeney, W. Zhang, I. McCulloch and D. M. DeLongchamp, *Nat Commun*, 2013, **4**, 2238.
10. Y. Li, W. K. Tatum, J. W. Onorato, Y. Zhang and C. K. Luscombe, *Macromolecules*, 2018, **51**, 6352-6358.
11. W. Zhong, S. Sun, L. Ying, F. Liu, L. Lan, F. Huang and Y. Cao, *ACS Appl. Mater. Interfaces*, 2017, **9**, 7315-7321.
12. A. Casey, Y. Han, Z. Fei, A. J. P. White, T. D. Anthopoulos and M. Heeney, *J. Mater. Chem. C*, 2015, **3**, 265-275.

13. W. Zhang, J. Smith, S. E. Watkins, R. Gysel, M. McGehee, A. Salleo, J. Kirkpatrick, S. Ashraf, T. Anthopoulos, M. Heeney and I. McCulloch, *J. Am. Chem. Soc.*, 2010, **132**, 11437-11439.

14. M. Planells, M. Nikolka, M. Hurhangee, P. S. Tuladhar, A. J. P. White, J. R. Durrant, H. Sirringhaus and I. McCulloch, *J. Mater. Chem. C*, 2014, **2**, 8789-8795.

15. M. Y. Lee, S. Dharmapurikar, S. J. Lee, Y. Cho, C. Yang and J. H. Oh, *Chem. Mater.*, 2020, **32**, 1914-1924.

16. F. Sugiyama, A. T. Kleinschmidt, L. V. Kayser, M. A. Alkhadra, J. M. Wan, A. S. Chiang, D. Rodriquez, S. E. Root, S. Savagatrup and D. J. Lipomi, *Macromolecules*, 2018, **51**, 5944-5949.

17. Y. C. Lin, F. H. Chen, Y. C. Chiang, C. C. Chueh and W. C. Chen, *ACS Appl. Mater. Interfaces*, 2019, **11**, 34158-34170.

18. B. O'Connor, E. P. Chan, C. Chan, B. R. Conrad, L. J. Richter, R. J. Kline, M. Heeney, I. McCulloch, C. L. Soles and D. M. DeLongchamp, *ACS Nano*, 2010, **4**, 7538-7544.

19. B. O'Connor, R. J. Kline, B. R. Conrad, L. J. Richter, D. Gundlach, M. F. Toney and D. M. DeLongchamp, *Adv. Funct. Mater.*, 2011, **21**, 3697-3705.

20. C. Y. Gao, M. Pei, H. J. Choi and H. Yang, *Adv. Funct. Mater.*, 2019, **29**.

21. C. Lu, W.-Y. Lee, X. Gu, J. Xu, H.-H. Chou, H. Yan, Y.-C. Chiu, M. He, J. R. Matthews, W. Niu, J. B. H. Tok, M. F. Toney, W.-C. Chen and Z. Bao, *Advanced Electronic Materials*, 2017, **3**.

22. J. Mun, G.-J. N. Wang, J. Y. Oh, T. Katsumata, F. L. Lee, J. Kang, H.-C. Wu, F. Lissel, S. Rondeau-Gagné, J. B. H. Tok and Z. Bao, *Adv. Funct. Mater.*, 2018, **28**.

23. Y. Zheng, G. J. N. Wang, J. Kang, M. Nikolka, H. C. Wu, H. Tran, S. Zhang, H. Yan, H. Chen, P. Y. Yuen, J. Mun, R. H. Dauskardt, I. McCulloch, J. B. H. Tok, X. Gu and Z. Bao, *Adv. Funct. Mater.*, 2019, **29**, 1905340.

24. K. Ditte, J. Perez, S. Chae, M. Hambsch, M. Al-Hussein, H. Komber, P. Formanek, S. C. B. Mannsfeld, A. Fery, A. Kiriy and F. Lissel, *Adv. Mater.*, 2021, **33**, e2005416.

25. H.-C. Wu, S. J. Benight, A. Chortos, W.-Y. Lee, J. Mei, J. W. F. To, C. Lu, M. He, J. B. H. Tok, W.-C. Chen and Z. Bao, *Chem. Mater.*, 2014, **26**, 4544-4551.

26. H. Ren, J. Zhang, Y. Tong, J. Zhang, X. Zhao, N. Cui, Y. Li, X. Ye, Q. Tang and Y. Liu, *J. Mater. Chem. C*, 2020, **8**, 15646-15654.

27. S. Y. Son, J.-H. Kim, E. Song, K. Choi, J. Lee, K. Cho, T.-S. Kim and T. Park, *Macromolecules*, 2018, **51**, 2572-2579.

28. Y. Li, W. K. Tatum, J. W. Onorato, S. D. Barajas, Y. Y. Yang and C. K. Luscombe, *Polym. Chem.*, 2017, **8**, 5185-5193.

29. H.-C. Wu, C.-C. Hung, C.-W. Hong, H.-S. Sun, J.-T. Wang, G. Yamashita, T. Higashihara and W.-C. Chen, *Macromolecules*, 2016, **49**, 8540-8548.

30. H.-F. Wen, H.-C. Wu, J. Aimi, C.-C. Hung, Y.-C. Chiang, C.-C. Kuo and W.-C. Chen, *Macromolecules*, 2017, **50**, 4982-4992.

31. J. Y. Oh, S. Rondeau-Gagne, Y. C. Chiu, A. Chortos, F. Lissel, G. N. Wang, B. C. Schroeder, T. Kurosawa, J. Lopez, T. Katsumata, J. Xu, C. Zhu, X. Gu, W. G. Bae, Y. Kim, L. Jin, J. W. Chung, J. B. Tok and Z. Bao, *Nature*, 2016, **539**, 411-415.

32. Y.-C. Lin, C.-C. Shih, Y.-C. Chiang, C.-K. Chen and W.-C. Chen, *Polym. Chem.*, 2019, **10**, 5172-5183.